Available online at www.giornaleitalianoendodonzia.it

ORIGINAL ARTICLE

Investigating the Efficacy of the Metal Artifact Reduction Algorithm in Cone-Beam Computed Tomography Images for Endodontic and Restorative Materials

ABSTRACT

Aim: *This study aimed to assess the effectiveness of metal artifact reduction (MAR) algorithms in cone-beam computed tomography (CBCT) images, specifically for various common dental materials. Metal restorations, posts, and gutta-percha frequently cause artifacts due to their high density, impacting image quality.*
Methodology: *Researchers used 11 extracted human mandibular teeth with different dental materials (amalgam, metal posts, porcelain-fused-to-metal (PFM) crowns, gutta-percha) and three intact teeth. CBCT scans were performed using a Galileos scanner on a mandible in water to simulate soft tissue. Images were acquired both with and without MAR activation across various tooth positions. Contrast-to-noise ratio (CNR) was calculated at multiple distances and angles. Statistical analysis was conducted using the Wilcoxon test.*
Results: *The study found that activating the MAR algorithm had no significant impact on reducing metal artifacts across any of the evaluated dental materials, regardless of tooth type, position, or angle.*
Conclusion: *The MAR algorithm, as tested, does not significantly reduce metal artifacts caused by dental materials like amalgam, metal posts, PFM crowns, or gutta-percha in CBCT images. In this context, clinical application of these algorithm does not provide justifiable added benefits.*

Mehrdad Abdinian[1]
Fateme Halvaei[2]
Mahsa Moannaei[3,*]
Parisa Soltani[1,4,5]
Carlo Rengo[4,§]
Mariangela Cernera[4,5,*,§]

[1] *Department of Oral and Maxillofacial Radiology, Dental Implants Research Center, Dental Research Institute, School of Dentistry, Isfahan University of Medical Sciences, Isfahan, Iran*
[2] *Student Research Committee, School of Dentistry, Isfahan University of Medical Sciences, Isfahan, Iran*
[3] *Department of Oral and Maxillofacial Radiology, School of Dentistry, Hormozgan University of Medical Sciences, Bandar Abbas, Iran.*
[4] *Department of Neurosciences, Reproductive and Odontostomatological Sciences, University of Naples 'Federico II', Naples, Italy.*
[5] *Department of Translational Medical Sciences, University of Naples 'Federico II', Naples, Italy.*

[§] *Carlo Rengo and Mariangela Cernera are co-last authors*

Received 2025, May 31
Accepted 2025, June 5

KEYWORDS *Cone beam computed tomography, artifacts, dental material.*

Corresponding Authors*
Mahsa Moannaei | Department of Oral and Maxillofacial Radiology, School of Dentistry, Hormozgan University of Medical Sciences, Bandar Abbas, Iran | email: Moannaei.mahsa@gmail.com | Mariangela Cernera | Department of Neurosciences, Reproductive and Odontostomatological Sciences, University of Naples 'Federico II', Naples, Italy | email: mariangela.cernera@icloud.com

Peer review under responsibility of Società Italiana di Endodonzia
10.32067/GIE.2025.523

Introduction

Cone-beam computed tomography (CBCT) is the main three-dimensional imaging modality for maxillofacial structures based on reconstruction from two-dimensional images (1). CBCT is a valuable tool in dental diagnosis and treatment planning (2-5). Previous evidence has shown that the presence of materials with high density and high atomic number leads to artifacts in the reconstructed images (6). A variety of restorative and endodontic materials are used in modern dentistry (7, 8), most of which contain radiopacifier agents to allow visualization in dental radiographs (9). Materials such as metal posts, metal restorations, dental implants, and metal crowns cause the formation of artifacts. These artifacts appear as shadows and lines on the adjacent structures (10, 11), thereby reducing the diagnostic utility of CBCT images (12). Metal artifact reduction (MAR) algorithms and image processing methods, developed with the aim of reducing potential image distortions, have been introduced to enhance the quality of CBCT images (13). However, significant variability in the results obtained by using these algorithms under different imaging conditions, such as variations in the type of material and its placement, has been observed, which calls into question the true interpretability of the images (14). Therefore, evaluating the effectiveness of MAR under different conditions appears to be essential. Different studies have focused on investigating the quantitative performance of MAR algorithms in CBCT images with controversial findings. Khosravifard et al. (15), using the Canny edge detection technique to quantify the amount of artifacts, found that MAR algorithms of their Vatech CBCT scanner significantly decreased the amount of artifacts arising from a titanium implant and a stainless steel intracanal post. Bechara et al. (16) used a phantom incorporating three metallic beads and three epoxy resin-based bone substitutes to simulate bone next to metal and concluded that MAR increased the contrast-to-noise ratio (CNR) in the presence of metal objects. Contrasting these results, Soltani et al. (17) reported that MAR algorithm of Genoray CBCT scanner was not successful in reducing the artifacts surrounding ceramic brackets and coated archwires. Queiroz et al. (6) concluded that while there was a significant reduction in artifacts surrounding dental alloys with MAR, no difference was detected in the artifacts around gutta-percha, regardless of MAR use (14). These findings reflect the diversity in the results of different studies performed on quantification of metallic artifacts arising from various dental materials. To the authors' knowledge, no study has been previously performed to investigate the efficacy of the native MAR algorithm of the Galileos CBCT scanner in reducing metallic artifacts surrounding a variety of different dental materials and in different conditions. Therefore, this study aimed to evaluate the efficacy of the MAR algorithm in CBCT images for various dental materials.

Material and Methods

Study Design and Setting

This ex-vivo study was performed on extracted human mandibular teeth. The study was ethically approved by the Research Ethics Committee, Isfahan University of Medical Sciences (#IR.MUI.RESEARCH.REC.1401.240). A sample size of 18 regions of interest (ROIs) was determined for this study. With this number of images, there is an 80% probability of detecting a difference equivalent to d = 0.93 (i.e., 0.93 times the standard deviation (SD)) between the mean CNR and SD values for the different materials at a significance level of α=0.05. Inclusion criteria were intact crowns without fracture, caries, or morphological abnormalities. The teeth were excluded if unnecessary loss of dental structures occurred during preparation. These teeth, five left first molars (36), five right first molars (46), and four left central incisors (31).

Sample Preparation

For each dental material, two posterior

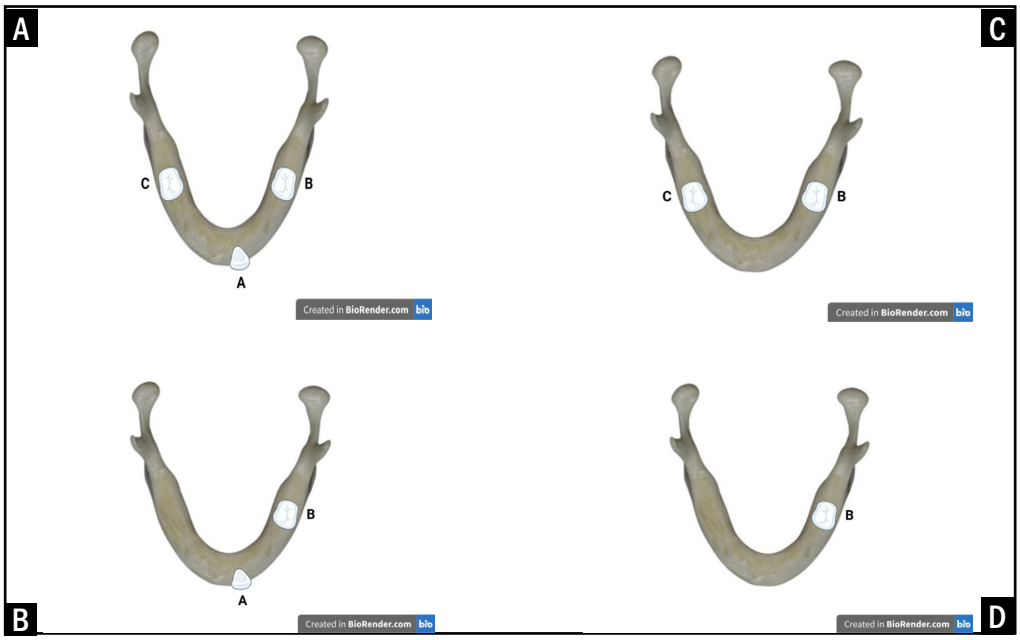

Figure 1
Schematic demonstration of positions of teeth in the mandible for CBCT imaging: (a) ABC position; (b) AB position; (c) BC position; and (d) B position (Created in https://BioRender.com).

teeth and one anterior tooth were selected, except for amalgam, for which only two posterior teeth were chosen. Initially, all teeth were disinfected in 70% alcohol, and any carious lesions were removed. Subsequently, each tooth was prepared for the application of the tested materials:

Gutta Percha: two left first molars, two right first molars, and two central incisors were selected. The canals of these teeth were instrumented to the appropriate length and width (18). The teeth were then obturated with gutta-percha points (Meta Biomed, Chungcheongbuk-do South Korea), using the lateral condensation technique. Three of the obturated teeth (36, 31, and 46) were chosen for the evaluation of the gutta-percha material.

Intracanal post: another three obturated teeth (36, 31, and 46) were designated for post placement. In the distal canals of teeth 36 and 46, as well as in the canal of tooth 31, the root canal filling material was removed first using Piezo #2 and then with Piezo #3 (Dentsply Maillefer, Ballaigues, Switzerland) up to a depth corresponding to two-thirds of the canal length. Following this, post-space impressions were taken and sent to the laboratory for the fabrication of cast posts. The cast posts were subsequently inserted into the corresponding canals, and the fit of the posts was verified using periapical radiography.

Porcelain fused to metal (PFM) crowns: an additional three teeth (31, 36, and 46) were selected for preparation for the placement of PFM crowns.

The incisal edge of the anterior tooth was reduced by 2 mm, and its labial and lingual surfaces were reduced by 1.2 mm and 0.8 mm, respectively. In the posterior teeth, the functional cusps were reduced by 2 mm, while the non-functional cusps were reduced by 1.5 mm.

The buccal and lingual surfaces of these posterior teeth were also reduced by 1.2 mm and 0.8 mm, respectively. After taking impressions, the crowns were cast and porcelain-fused-to-metal restorations were fabricated in the laboratory. The crowns were then placed on the respective teeth, and the adaptation of the crown margins to the teeth was evaluated using periapical radiography and a probe.

Amalgam restoration: lastly, an MOD cavity was prepared on two posterior teeth (36 and 46) and restored with amalgam (Cinalux, Tehran, Iran).

The mandible was fixed at the bottom of a plastic container using wax; to simulate soft tissue conditions, the container was then filled with a mixture of water and oil.

CBCT Image Acquisition: the mounting positions are schematically shown in Fig-

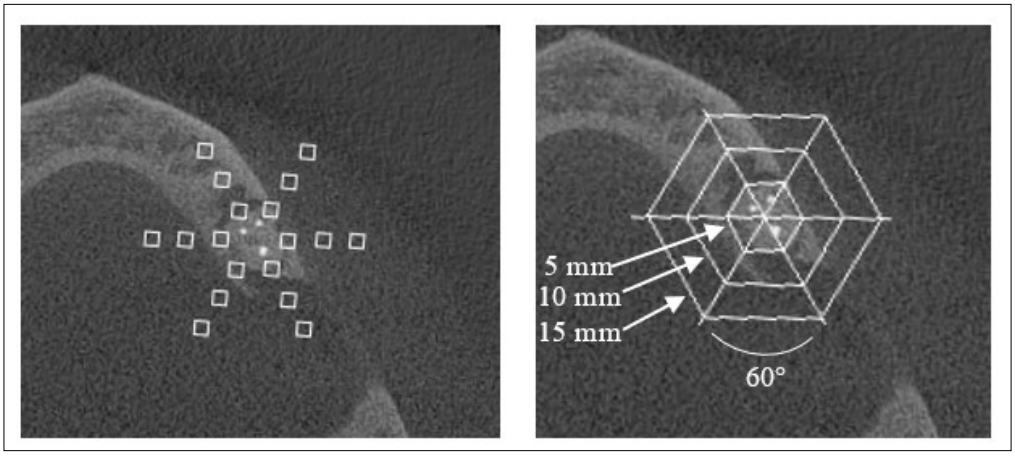

Figure 2
ROIs and their position in the CBCT axial image

ure 1. For gutta-percha, posts, PFM crowns, and the intact teeth, CBCT scans were performed in three positions:
ABC Position: All three teeth were present.
AB Position: Only teeth 31 and 36 were present.
B Position: Only tooth 36 was present.
For amalgam, scans were performed in two positions:
BC Position: Both teeth 36 and 46 were present.
B Position: Only tooth 36 was present.
For each material in each position, four CBCT images were acquired. The procedure involved taking two images without activating the MAR algorithm, and then two images with activation of the MAR. The CBCT scan was repeated twice to address any variability in image acquisition. All images were acquired using the Galileos CBCT scanner (Sirona, Bensheim, Germany) with exposure parameters set at 85 kVp and 21 mAs, voxel size 280 micrometers, and field of view 15 cm×15 cm.

CBCT Image Analysis
The DICOM files generated from the CBCT scans were imported into ImageJ software (NIH, Bethesda, MD, USA). In a preselected axial image, 18 square-shaped ROIs with dimensions of 2 mm × 2 mm were created. This was achieved by dividing the area surrounding each tooth into six segments using lines drawn at 60-degree intervals. Additionally, three circular sections with radii of 5, 10, and 15 mm were drawn centered on the tooth, and the intersection points of these lines and circles were designated as the ROIs (Figure 2). For each ROI, the mean and SD of the gray values were calculated.
To calculate the CNR, an ROI of similar size was selected in the water surrounding the mandible, and the mean and SD of the gray value were recorded as a control. The CNR was calculated as follows:

$$NR = \frac{|Mean - Mean_{control}|}{\sqrt{SD^2 + SD^2_{control}}}$$

Data analysis was performed using the Wilcoxon test (α=0.05) by the Statistical Package for the Social Sciences (SPSS, version 26, IBM Statistics, Armonk, NY, USA).

Results

For each dental material, two posterior teeth and one anterior tooth were selected, except for amalgam, for which only two posterior teeth were chosen. Additionally, four CBCT images were obtained in each of the positions (two with and two without activation of MAR). For the amalgam restoration, when only one posterior tooth was present (position B), there was no significant difference between CNR values in the MAR activated and deactivated conditions, at distances of 5 mm (P=0.248), 10 mm (P=0.248), and 15 mm (P=0.463) from the center of the tooth (overall P=0.679). Similarly, when two posterior teeth were present (position BC), there was no significant difference between CNR

Table 1

Mean (SD) of CNR values of teeth in the presence of amalgam restorations.

Position	Distance	MAR	Number	Mean (SD)	P-value
B	5 mm	Off	6	1.571 (0.763)	0.248
		On	6	1.390 (0.812)	
	10 mm	Off	6	27.374 (6.274)	0.248
		On	6	27.392 (6.286)	
	15 mm	Off	6	19.733 (5.565)	0.463
		On	6	19.718 (5.271)	
	Total	Off	18	16.226 (11.969)	0.679
		On	18	16.167 (12.514)	
BC (for left molar)	5 mm	Off	6	1.446 (0.669)	0.172
		On	6	1.464 (0.647)	
	10 mm	Off	6	24.857 (4.635)	0.248
		On	6	24.839 (4.717)	
	15 mm	Off	6	21.964 (6.347)	0.463
		On	6	21.969 (6.318)	
	Total	Off	18	16.895 (11.481)	0.711
		On	18	16.913 (11.465)	

values of MAR activated and deactivated conditions, at distances of 5 mm (P=0.172), 10 mm (P=0.248), and 15 mm (P=0.463) from the center of the left molar (overall P=0.711) (Table 1).

For the gutta-percha material, when all three teeth were present (position ABC), there was no significant difference between the CNR values of the left anterior incisor in active and inactive MAR conditions at distances of 5 mm (P=0.753), 10 mm (P=0.172), and 15 mm (P=0.463) from the center of the tooth (overall P=0.982). Similarly, for the left molar, when all three teeth were present (position ABC), there was no significant difference between CNR values of MAR activated and deactivated conditions, at distances of 5 mm (P=0.600), 10 mm (P=0.916), and 15 mm (P=0.753) from the center of the tooth (overall P=0.810). The same results were found in AB position for the left central incisor (P=0.753, P=0.753, P=0.600, and P=0.982 for 5-, 10-, and 15-mm distances and overall, respectively) and left molar (P=0.345, P=0.248, P=0.172, and P=0.420 for 5-, 10-, and 15-mm distances and overall, respectively). In presence of the left molar (position B), there was no significant difference between CNR values of MAR activated and deactivated conditions, at distances of 5 mm (P=0.463), 10 mm (P=0.248), and 15 mm (P=0.916) from the center of the tooth (overall P=0.878) (Table 2).

For the PFM crowns, when all three teeth were present (position ABC), there was no significant difference between the CNR values of the left anterior incisor in active and inactive MAR conditions at distances of 5 mm (P=0.600), 10 mm (P=0.175), and 15 mm (P=0.753) from the center of the tooth (overall P=0.472). Similarly, for the left molar, when all three teeth were pres-

Table 2

Mean (SD) of CNR values of teeth in the presence of gutta-percha.

Position	Distance	MAR	Number	Mean (SD)	P-value
ABC (for left central incisor)	5 mm	Off	6	17.957 (4.706)	0.753
		On	6	17.940 (4.681)	
	10 mm	Off	6	19.844 (2.143)	0.172
		On	6	19.824 (2.415)	
	15 mm	Off	6	22.612 (3.595)	0.463
		On	6	22.628 (3.597)	
	Total	Off	18	19.850 (4.108)	0.982
		On	18	19.849 (4.103)	
ABC (for left molar)	5 mm	Off	6	13.127 (3.963)	0.600
		On	6	12.603 (3.405)	
	10 mm	Off	6	17.788 (1.784)	0.916
		On	6	17.800 (1.762)	
	15 mm	Off	6	15.453 (3.757)	0.753
		On	6	15.452 (3.738)	
	Total	Off	18	15.456 (3.680)	0.810
		On	18	15.285 (3.635)	
AB (for left central incisor)	5 mm	Off	6	22.935 (3.243)	0.753
		On	6	22.945 (3.325)	
	10 mm	Off	6	22.270 (2.884)	0.753
		On	6	22.179 (2.918)	
	15 mm	Off	6	22.121 (1.453)	0.600
		On	6	22.107 (1.377)	
	Total	Off	18	22.352 (2.375)	0.982
		On	18	22.351 (2.379)	
AB (for left molar)	5 mm	Off	6	1.963 (3.339)	0.345
		On	6	1.646 (3.136)	
	10 mm	Off	6	15.315 (2.636)	0.248
		On	6	15.297 (2.649)	
	15 mm	Off	6	18.691 (3.617)	0.172
		On	6	18.709 (3.621)	
	Total	Off	18	14.700 (4.673)	0.420
		On	18	14.690 (4.688)	
B	5 mm	Off	6	1.539 (2.247)	0.463
		On	6	1.552 (2.214)	
	10 mm	Off	6	15.504 (1.913)	0.248
		On	6	15.488 (1.894)	
	15 mm	Off	6	17.116 (2.650)	0.916
		On	6	17.124 (2.671)	
	Total	Off	18	14.386 (3.594)	0.878
		On	18	14.388 (3.586)	

Table 3

Mean (SD) of CNR values of teeth in the presence of PFM restorations.

Position	Distance	MAR	Number	Mean (SD)	P-value
ABC (for left central incisor)	5 mm	Off	6	17.813 (4.598)	0.600
		On	6	17.825 (4.605)	
	10 mm	Off	6	2.854 (4.264)	0.175
		On	6	2.827 (4.830)	
	15 mm	Off	6	17.637 (2.522)	0.753
		On	6	17.634 (2.513)	
	Total	Off	18	18.767 (3.894)	0.472
		On	18	18.762 (3.884)	
ABC (for left molar)	5 mm	Off	6	1.320 (0.655)	0.463
		On	6	1.307 (0.648)	
	10 mm	Off	6	2.239 (4.552)	0.753
		On	6	2.251 (4.507)	
	15 mm	Off	6	18.826 (7.372)	0.600
		On	6	18.830 (7.156)	
	Total	Off	18	13.462 (9.959)	0.810
		On	18	13.462 (9.957)	
AB (for left central incisor)	5 mm	Off	6	17.827 (4.425)	0.248
		On	6	17.796 (4.393)	
	10 mm	Off	6	18.294 (5.287)	0.600
		On	6	18.309 (5.320)	
	15 mm	Off	6	18.424 (3.585)	0.753
		On	6	18.425 (3.601)	
	Total	Off	18	18.182 (4.223)	0.743
		On	18	18.177 (4.230)	
AB (for left molar)	5 mm	Off	6	1.479 (1.246)	0.753
		On	6	1.494 (1.203)	
	10 mm	Off	6	18.376 (6.645)	0.248
		On	6	18.392 (6.663)	
	15 mm	Off	6	17.885 (5.703)	0.916
		On	6	17.888 (5.691)	
	Total	Off	18	12.580 (9.396)	0.327
		On	18	12.591 (9.394)	
B	5 mm	Off	6	1.232 (1.155)	0.463
		On	6	1.228 (1.128)	
	10 mm	Off	6	18.577 (5.487)	0.753
		On	6	18.579 (5.496)	
	15 mm	Off	6	17.364 (6.582)	0.463
		On	6	17.379 (6.539)	
	Total	Off	18	12.391 (9.390)	0.711
		On	18	12.395 (9.386)	

ent (position ABC), there was no significant difference between CNR values of MAR activated and deactivated conditions, at distances of 5 mm (P=0.463), 10 mm (P=0.753), and 15 mm (P=0.600) from the center of the tooth (overall P=0.810). The same results were found in AB position for the left central incisor (P=0.248, P=0.600, P=0.753, and P=0.743 for 5-, 10-, and 15-mm distances and overall, respectively) and left molar (P=0.753, P=0.248, P=0.916, and P=0.327 for 5-, 10-, and 15-mm distances and overall, respectively). In presence of the left molar (position B), there was no significant difference between CNR values of MAR activated and deactivated conditions, at distances of 5 mm (P=0.463), 10 mm (P=0.753), and 15 mm (P=0.463) from the center of the tooth (overall P=0.711) (Table 3). For the intracanal posts, when all three teeth were present (position ABC), there was no significant difference between the CNR values of the left anterior incisor in active and inactive MAR conditions at distances of 5 mm (P=0.600), 10 mm (P=0.248), and 15 mm (P=0.600) from the center of the tooth (overall P=0.248). Similarly, for the left molar, when all three teeth were present (position ABC), there was no significant difference between CNR values of MAR activated and deactivated conditions, at distances of 5 mm (P=0.600), 10 mm (P=0.916), and 15 mm (P=0.115) from the center of the tooth (overall P=0.111). The same results were found in AB position for the left central incisor (P=0.248, P=0.248, P=0.753, and P=0.943 for 5-, 10-, and 15-mm distances and overall, respectively) and left molar (P=0.463, P=0.345, P=0.345, and P=0.844 for 5-, 10-, and 15-mm distances and overall, respectively). In presence of the left molar (position B), there was no significant difference between CNR values of MAR activated and deactivated conditions, at distances of 5 mm (P=0.248), 10 mm (P=0.345), and 15 mm (P=0.916) from the center of the tooth (overall P=0.947) (Table 4).

Discussion

The present study investigated the effectiveness of the MAR algorithm in CBCT images for dental materials, including amalgam, metal posts, PFM crowns, and gutta-percha, and it was observed that there was no significant difference in the mean CNR between the two conditions (MAR activated and deactivated) for any of the dental materials or at any of the evaluated distances and positions.

In 2020, Fontenele et al. (1) performed CBCT scans on a human mandible—once with a zirconia implant and once without—under three MAR conditions (no MAR, MAR before exposure, and MAR after exposure). Artifacts in the ROIs were measured at various distances and angles relative to the implant using SD and CNR. They concluded that both MAR conditions reduce the amount of artifacts in CBCT images, particularly when artifact effects are more pronounced. This finding contrasts with the present study's results; the discrepancy may be due to differences in the material type under investigation.

Kim et al. (19), in 2020, used four phantoms fitted with prostheses made of amalgam, gold, zirconia, and PFM. They acquired CBCT images both with and without MAR activation, as well as under different settings: kVp values of 100 and 70, and voxel sizes of 0.2 mm and 0.3 mm. They concluded that the MAR algorithm reduces the extent of streaked artifacts, but its effect depends on the device settings and the type of prosthesis. The differences in results can be attributed to the fact that the present study did not consider the role of exposure settings. In 2022, Farias-Gomes et al. (20) investigated the effect MAR algorithm in various regions of teeth restored with different posts, and they found that for nickel-chromium and chrome-cobalt posts, these algorithms do not lead to a significant reduction in artifact levels in the different regions. In general, the findings of that study are consistent with those of the present study. The present study aimed to evaluate the effectiveness of the MAR algorithm in CBCT images for various dental materials. The findings of this study, regarding lack of significant efficacy of Galileos scanner's native MAR algorithm, prompts further consideration of several factors that may influence both artifact formation and the efficacy of artifact reduction algorithms. A critical factor that may account for the lack

Table 4

Mean (SD) of CNR values of teeth in the presence of intracanal post restorations.

Position	Distance	MAR	Number	Mean (SD)	P-value
ABC (for left central incisor)	5 mm	Off	6	16.519 (2.414)	0.600
		On	6	16.523 (2.394)	
	10 mm	Off	6	17.694 (4.192)	0.248
		On	6	17.902 (4.158)	
	15 mm	Off	6	17.873 (3.943)	0.600
		On	6	17.883 (3.912)	
	Total	Off	18	17.154 (3.432)	0.248
		On	18	17.165 (3.413)	
ABC (for left molar)	5 mm	Off	6	6.525 (3.865)	0.600
		On	6	6.523 (3.842)	
	10 mm	Off	6	16.698 (4.182)	0.916
		On	6	16.701 (4.200)	
	15 mm	Off	6	14.801 (3.228)	0.115
		On	6	14.775 (3.239)	
	Total	Off	18	12.675 (5.767)	0.111
		On	18	12.666 (5.068)	
AB (for left central incisor)	5 mm	Off	6	19.297 (3.174)	0.248
		On	6	19.557 (3.089)	
	10 mm	Off	6	16.829 (5.861)	0.248
		On	6	16.814 (5.848)	
	15 mm	Off	6	17.927 (3.002)	0.753
		On	6	17.921 (2.964)	
	Total	Off	18	17.933 (4.652)	0.943
		On	18	17.930 (4.668)	
AB (for left molar)	5 mm	Off	6	8.497 (5.163)	0.463
		On	6	8.505 (5.161)	
	10 mm	Off	6	16.255 (1.610)	0.345
		On	6	16.274 (1.639)	
	15 mm	Off	6	14.866 (6.960)	0.345
		On	6	14.850 (6.117)	
	Total	Off	18	13.206 (5.622)	0.844
		On	18	13.211 (5.629)	
B	5 mm	Off	6	6.518 (3.430)	0.248
		On	6	6.533 (3.421)	
	10 mm	Off	6	16.952 (3.527)	0.345
		On	6	16.802 (3.510)	
	15 mm	Off	6	14.412 (3.201)	0.916
		On	6	14.411 (2.964)	
	Total	Off	18	12.341 (5.312)	0.947
		On	18	12.341 (5.292)	

of significant differences in our study is the role of exposure parameters. Our investigation maintained fixed exposure settings (85 kVp and 21 mAs), similar to other studies where such conditions remained constant. In contrast, it is revealed that variations in kVp, mAs, and even voxel sizes can alter artifact production, thereby affecting the performance of MAR algorithms (19). This brings into focus the importance of optimizing exposure settings combined with MAR activation to potentially enhance image quality. The rapid development of new radiology programs, along with the fast-paced advancement in image processing techniques, has led to an increased demand for customizable image analysis software. ImageJ is a free image processing software capable of handling DICOM format images and is supported by the National Institutes of Health. This software serves as a powerful platform for image processing, offering users a wide range of tools for comprehensive image analysis (21). Among the limitations of the present study is its laboratory-based nature. The findings of this study should be further examined in subsequent stages using CBCT images acquired from patients. In addition, employing only one MAR algorithm in this study makes direct comparison between different algorithms difficult. As an integral part of digital dentistry, CBCT imaging is an ever-evolving field (22). With the rapid improvements in the field of artificial intelligence (AI), a promising avenue for further research is applying AI-based approaches for correcting metallic artifacts and improving the image quality in CBCT images. Therefore, further research investigating the effects of these modern AI-driven methods on the amount of artifacts caused by different endodontic and restorative materials is recommended.

Conclusion

The activation of the MAR algorithm does not significantly reduce metal artifacts for dental materials such as amalgam, metal posts, PFM crowns, and gutta-percha. In this context, clinical application of these algorithm does not provide justifiable added benefits.

Funding

This work was funded by Isfahan University of Medical Sciences (#3401405).

Referencess

1. *Fontenele RC, Nascimento EHL, Santaella GM, Freitas DQ. Does the metal artifact reduction algorithm activation mode influence the magnitude of artifacts in CBCT images? Imaging Sci Dent. 2020;50(1):23-30.*
2. *Mehdizadeh M, Booshehri SG, Kazemzadeh F, Soltani P, Motamedi MRK. Level of knowledge of dental practitioners in Isfahan, Iran about cone-beam computed tomography and digital radiography. isd. 2015;45(2):133-5.*
3. *Oprea B, Iuga MM, Salgado FME, Teja KV, Grila A, Herschbach D, et al. Successful treatment of a damaged upper molar using 3D Technology: a case report with 4 years follow-up: CAD-CAM technology in endodontics. Giornale Italiano di Endodonzia. 2024;38(3).*
4. *Garcia-Sanchez A, Sato M, Gargano A, Nasir M, Pita A, Mateos-Moreno M-V, et al. A comparison in the efficacy of 3D-printed guides versus traditional endodontic access: an ex-vivo study. Giornale Italiano di Endodonzia. 2024;38(3).*
5. *Hénaut M, Meire M, Vandomme J, Robberecht L. Evaluation of Cone Beam Computed Tomography Resolution, 3D Printing Resolution and Drilling Depth on Drilling Accuracy in Guided Endodontics: An In-Vitro Study. European Endodontic Journal. 2025;10(2):127-33.*
6. *Queiroz PM, Oliveira ML, Groppo FC, Haiter-Neto F, Freitas DQ. Evaluation of metal artefact reduction in cone-beam computed tomography images of different dental materials. Clin Oral Investig. 2018;22(1):419-23.*
7. *Spagnuolo G. Bioactive dental materials: the current status. MDPI; 2022. p. 2016.*
8. *Cadenaro M, Josic U, Maravić T, Mazzitelli C, Marchesi G, Mancuso E, et al. Progress in dental adhesive materials. Journal of dental research. 2023;102(3):254-62.*
9. *Lin H-N, Chen W-W, Hsu C-C, Chen M-S, Chang P-J, Chang W-M, et al. Endodontic Radiopacifying Application of Barium Titanate Prepared through a Combination of Mechanical Milling and Heat Treatment. Materials. 2023;16(23):7270.*
10. *Coelho-Silva F, Martins LAC, Braga DA, Zandonade E, Haiter-Neto F, de-Azevedo-Vaz SL. Influence of windowing and metal artefact reduction algorithms on the volumetric dimensions of five different high-density materials: a cone-beam CT study. Dentomaxillofac Radiol. 2020;49(8):20200039.*
11. *Vasconcelos KF, Codari M, Queiroz PM, Nicolielo LFP, Freitas DQ, Sforza C, et al. The performance of metal artifact reduction algorithms in cone beam computed tomography images considering the effects of materials, metal positions, and fields of view. Oral Surg Oral Med Oral Pathol Oral Radiol. 2019;127(1):71-6.*
12. *Sheikhi M, Behfarnia P, Mostajabi M, Nasri N. The efficacy of metal artifact reduction (MAR) algorithm*

in cone-beam computed tomography on the diagnostic accuracy of fenestration and dehiscence around dental implants. J Periodontol. 2020;91(2):209-14.
13. *Queiroz PM, Groppo FC, Oliveira ML, Haiter-Neto F, Freitas DQ. Evaluation of the efficacy of a metal artifact reduction algorithm in different cone beam computed tomography scanning parameters. Oral Surg Oral Med Oral Pathol Oral Radiol. 2017;123(6):729-34.*
14. *de Faria Vasconcelos K, Queiroz PM, Codari M, Pinheiro Nicolielo LF, Freitas DQ, Jacobs R, et al. A quantitative analysis of metal artifact reduction algorithm performance in volume correction with 3 CBCT devices. Oral Surg Oral Med Oral Pathol Oral Radiol. 2020;130(3):328-35.*
15. *Khosravifard A, Saberi BV, Khosravifard N, Motallebi S, Kajan ZD, Ghaffari ME. Application of an auto-edge counting method for quantification of metal artifacts in CBCT images: a multivariate analysis of object position, field of view size, tube voltage, and metal artifact reduction algorithm. Oral Surgery, Oral Medicine, Oral Pathology and Oral Radiology. 2021;132(6):735-43.*
16. *Bechara BB, Moore WS, McMahan CA, Noujeim M. Metal artefact reduction with cone beam CT: an in vitro study. Dentomaxillofac Radiol. 2012;41(3):248-53.*
17. *Soltani P, Cernera M, Kachuie M, Moaddabi A, Khoramian M, Spagnuolo G, et al. Efficacy of a Metal Artifact Reduction Algorithm in CBCT Images of Teeth With Ceramic Brackets With/Without Coated Archwires: An In Vitro Study. Clinical and Experimental Dental Research. 2025;11(1):e70112.*
18. *Abdinian M, Moshkforoush S, Hemati H, Soltani P, Moshkforoushan M, Spagnuolo G. Comparison of cone beam computed tomography and digital radiography in detecting separated endodontic files and strip perforation. Applied Sciences. 2020;10(23):8726.*
19. *Kim YH, Lee C, Han S-S, Jeon KJ, Choi YJ, Lee A. Quantitative analysis of metal artifact reduction using the auto-edge counting method in cone-beam computed tomography. Scientific Reports. 2020;10(1):8872.*
20. *Farias-Gomes A, Fontenele RC, Rosado LPL, Neves FS, Freitas DQ. The metal post material influences the performance of artefact reduction algorithms in CBCT images. Braz Dent J. 2022;33(1):31-40.*
21. *Rueden CT, Schindelin J, Hiner MC, DeZonia BE, Walter AE, Arena ET, et al. ImageJ2: ImageJ for the next generation of scientific image data. BMC Bioinformatics. 2017;18(1):529.*
22. *Spagnuolo G, Sorrentino R. The role of digital devices in dentistry: clinical trends and scientific evidences. MDPI; 2020. p. 1692.*